Food Chemistry: X 26 (2025) 102301

Contents lists available at ScienceDirect

Food Chemistry: X

journal homepage: www.sciencedirect.com/journal/food-chemistry-x

Flavonoids profile and antioxidant capacity of four wine grape cultivars and their wines grown in the Turpan Basin of China, the hottest wine region in the world

Shijian Bai [a,b,1], Xiaoqing Tao [a,1], Jinge Hu [b,*], Huawei Chen [a], Jiuyun Wu [c], Fuchun Zhang [d], Junshe Cai [b], Guohong Wu [b,*], Jiangfei Meng [a,*]

[a] College of Enology, Northwest A&F University, Yangling, Shaanxi 712100, China
[b] Xinjiang Uygur Autonomous Region Research and Development Center for Protected Agriculture and Characteristic Agriculture, Shanshan, Xinjiang 838200, China
[c] Turpan Experimental Station, Xinjiang Academy of Agricultural Sciences, Turpan, Xinjiang 83800, China
[d] Institute of Horticulture Crops, Xinjiang Academy of Agricultural Sciences, Urumqi 830091, China

ARTICLE INFO

Keywords:
Grape berry
Wine
Anthocyanidins
Flavonoids
Hottest wine region

ABSTRACT

This study analyzed the flavonoid profiles and antioxidant capacities of berries and wines from four wine grape cultivars (*Vitis vinifera* cv. Cabernet Sauvignon, Marselan, Saperavi, and Syrah) cultivated in the Turpan Basin, the hottest wine region globally. A total of 43 anthocyanins and 66 non-anthocyanin flavonoids were identified using ultra-high performance liquid chromatography (UPLC-MS^E). Combining ABTS, DPPH and FRAP assays, Saperavi showed the highest anthocyanin concentration, contributing to its intense color, while Cabernet Sauvignon exhibited the strongest antioxidant capacity. Additionally, Syrah demonstated the highest retention of flavonols and flavan-3-ols during winemaking, enhancing its antioxidant properties. The flavonoid composition and antioxidant response patterns differed across cultivars. Marselan presented a balanced flavonoid profile, with moderate levels of anthocyanins and other flavonoids, resulting in stable color and antioxidant performance. These findings provide insight into varietal adaptability and biochemical performance under extreme high-temperature conditions, which are valuable for viticultural strategies in hot regions.

1. Introduction

The quality of wine is influenced by a complex interplay of various factors, primarily including grape cultivars, terroir conditions, and cultivation practices. Regional characteristics are particularly significant, as they are profoundly affected by environmental variables such as temperature, soil composition, and light intensity(Mezzatesta, Berli, Arancibia, Buscema, & Piccoli, 2022; Valentini et al., 2022). Among these influential factors, phenolic compounds, particularly flavonoids, play a crucial role in shaping the color, flavor profile, taste attributes, and antioxidant capacity of wine. The biosynthesis and accumulation of flavonoids are intricately linked to environmental conditions, highlighting the necessity for regional studies to examine their impact on wine quality (Yue et al., 2021).

The Turpan Basin, located in eastern Xinjiang, China, is recognized as one of the hottest wine regions globally, where extreme climatic conditions profoundly influence grape growth and the winemaking process. This region is characterized by a characteristic continental desert climate, marked by minimal precipitation, high evaporation rates, extremely arid air, and peak temperatures reaching 48 °C; it has been aptly termed the 'melting pot' (Zhang et al., 2020). These distinctive climatic attributes not only influence the physiology and metabolism of grapes but also play a crucial role in shaping the chemical composition and sensory characteristics of wine. Consequently, conducting a comprehensive investigation into the performance of various grape cultivars in such an extreme environment, particularly regarding their phenolic compound structure and antioxidant capacity, is essential for optimizing vineyard management practices.

Climatic factors, particularly temperature, precipitation, and sunshine duration, are critical determinants that influence grape growth, ripening, and chemical composition. Elevated temperature can accelerate grape ripening and potentially enhance the maturity and

* Corresponding author.
E-mail addresses: hujinge2007@163.com (J. Hu), xjptmmgs@126.com (G. Wu), mjfwine@nwafu.edu.cn (J. Meng).
[1] These authors contribute equality to this manuscript

https://doi.org/10.1016/j.fochx.2025.102301
Received 13 November 2024; Received in revised form 17 February 2025; Accepted 18 February 2025
Available online 21 February 2025

antioxidant activity of phenolic compounds (Rodríguez-Lorenzo et al., 2023). However, excessive heat can lead to reduced acidity and overripeness, creating an imbalance between sugar levels and acidity. This imbalance adversely affects both the quality and aging potential of wine, ultimately impacting the balance and flavor profile of the final product (Mosedale, Wilson, & Maclean, 2015). Under such environmental stressors, grapevines exhibit remarkable adaptive mechanisms by regulating the synthesis of phenolic compounds, thereby yielding wines with distinct characteristics.

Phenolic compounds in grapes have received considerable attention due to their significant impact on the sensory properties and health benefits of wine (He et al., 2012a). Flavonoids, the predominant phenolic compounds found in grapes, include flavonols, flavan-3-ols, and anthocyanins, all of which play crucial roles in determining the color, bitterness, and astringency of wine (Teixeira, Eiras-Dias, Castellarin, & Gerós, 2013). Moreover, these compounds are linked to various health benefits, including anti-inflammatory, anti-cancer, and cardiovascular protective effects (Kennedy, Saucier, & Glories, 2006). Anthocyanins, a key component of red wine, are primarily responsible for its color and significantly contribute to specific taste attributes. Their synthesis and accumulation are influenced by factors including grape maturity, environmental conditions, and grape variety. Despite the extensive research conducted in traditional wine regions, a comprehensive understanding of flavonoid dynamics in extreme climates, such as the Turpan Basin, remains limited. Therefore, investigating the flavonoid composition and antioxidant capacity of different grape cultivars within this region may elucidate the impact of its unique terroir on wine quality.

Research has demonstrated a significant correlation between polyphenol content and the antioxidant capacity of wine. These compounds are essential for protecting against ultraviolet radiation and combating pathogens, particularly in regions exposed to high levels of solar radiation, such as Turpan (Cohen, Tarara, Kennedy, & c. a., 2008). The extreme temperatures and intense sunlight characteristic of the Turpan Basin may promote increased concentrations of flavonoids in local grape cultivars, thereby enhancing wine quality. As the Chinese wine industry evolves, there is an increasing demand for wines that reflect distinct regional characteristics. Consequently, addressing the research gap regarding grape varietals cultivated under extreme conditions—such as those found in the Turpan Basin—is imperative for understanding the performance of different cultivars in this challenging environment and for enhancing the quality and uniqueness of wines produced in the region.

Given the distinctive climatic conditions of the Turpan Basin in Xinjiang, China, this study aims to analyze the performance of four primary wine grape cultivars in the region, including both internationally recognized and regionally endemic cultivars. The focus of this study is on the structure and antioxidant capacity of their phenolic compounds. This research aims to provide valuable insights into the selection and optimization of grape cultivars, ultimately supporting the production of high-quality wines that reflect the unique terroir characteristics of Turpan.

2. Material and methods

2.1. Chemicals and reagents

Methanol (chromatography grade) and acetonitrile (chromatography grade) were obtained from Merck. Formic acid (chromatography grade) was obtained from Sigma-Aldrich. Hydrochloric acid (analytical grade) was obtained from Xinyang Chemical Reagent Factory, and the corresponding standard of anthocyanin substances was acquired from isoReag (50 % methanol preparation, 1 mg/mL). The standard for non-anthocyanin flavonoids was obtained from MCE (70 % methanol formulation, 10 mmol/L).

2.2. Experimental location and treatment

This study focuses on Shanshan County, Turpan City, Xinjiang, China (geographical location: 42°87′ N, 90°33′ E, average altitude of 334.45 m). The annual rainfall in this region is only 25.3 mm, while the annual evaporation is as high as 2751 mm. The annual sunshine duration is 3122.8 h, the effective accumulated temperature exceeds 525 °C (calculated as greater than 10 °C), and the frost-free period lasts 192 days. Meteorological data were obtained from the National Earth System Science Data Center(https://www.geodata.cn/).

The four grape cultivars included are: Marselan (*Vitis vinifera*, Msl) and Syrah *(Vitis vinifera*, Sr) both planted in 2016, and Cabernet Sauvignon *(Vitis vinifera*, CS) and Saperavi *(Vitis vinifera,* Spr), both planted in 2011. All cultivars are own-rooted. The vineyards employ a consistent management approach, characterized by a fixed row spacing of 1.0 m × 3.5 m. The vines are oriented in a south-north direction and are supplemented by a drip irrigation system. Grape pruning adheres to a modified vertical shoot positioning (VSP) grid system. Each vine was pruned to retain 18–22 shoots and 27–33 clusters. Three rows of adjacent, uniform vines were selected for the experiment in each vineyard. Three replicate groups of 50 consecutive vines, each arranged in a row, were used for sampling.

2.3. Winemaking protocol

Grapes are selected, stemmed, and crushed before being placed in glass jars. A concentration of 60 mg/L SO_2 (added in the form of potassium metabisulfite, $K_2S_2O_5$) must be added immediately after crushing. Subsequently, 0.4 g pectinase was added and yeast strains prerehydrated according to the manufacturer's guidelines (Zymasil, AEB Group SpA, Bologna, Italy) were introduced to initiate the fermentation process. Under controlled conditions at a constant temperature of 26–28 °C, the skins were macerated and fermented with alcohol. The cap was manually released twice a day to release the accumulated carbon dioxide, and the mixture was agitated to promote even fermentation. The end of alcohol fermentation is marked when the concentration of reducing sugar is detected to drop below 4 g/L. The arcane wine (i.e., the wine that naturally flows out without pressing) is separated and placed under static conditions for natural clarification. The clarified wine is transferred to a 10-l glass container and aged at a suitable temperature of 20 °C for 20 days after adjusting the free SO_2 concentration to 40 mg/L to ensure the stability and safety of the wine. The samples are subsequently bottled and stored in a controlled low-temperature environment at −4 °C for further analysis. This specific temperature helps maintain the chemical composition of the wine samples in a stable condition until the analytical procedures can be conducted.

2.4. Physiochemical parameter of grapes and wines

The total soluble solids (TSS) of fruit juice were rapidly determined using portable refractometer (PAL-1, Aiya, Japan). The pH of fruit juice and wine is precisely measured with a state-of-the-art pH meter (LE438, Mettler-Toledo, Switzerland). The titrable acidity (TA) of fruit juice was measured by titration with a standard 0.05 mol/L NaOH solution using 1 % phenolphthalein dissolved in 75 % ethanol as an indicator. The reducing sugar content in fruit juice and wine was determined according to the National Standard of the People's Republic of China (GB 5009.7–2016). The alcohol concentration of the wine is accurately determined following the national standard (GB/T 15038–2006).

2.5. Measurement of chromatic parameters

Two mL of wine sample was filtered using a 0.45 μm polyethersulfone filter (Jinteng Experimental Equipment Co., Ltd., Tianjin, China), and the filter was added to a 2 mm path-length quartz cuvette. The wine's CIELab parameters were analyzed on a SP-756P

spectrophotometer (Shanghai spectrum, Shanghai, China) with distilled water as a reference. The parameters analyzed were brightness (L*), red/green value (a*), and yellow/blue value (b*). The chroma saturation (C*ab), hue angle (h*ab), and color difference (ΔEab) were calculated using Eqs. (1)–(3)(Pérez-Magariño & González-Sanjosé, 2003):

$$C^*ab = \left((\Delta a^*)^2 + (\Delta b^*)^2\right)^{1/2} \quad (1)$$

$$h^*ab = tan^{-1}\left(b^*/a^*\right) \quad (2)$$

$$\Delta Eab = \left((\Delta L^*)^2 + (\Delta a^*)^2 + (\Delta b^*)^2\right)^{1/2} \quad (3)$$

2.6. Detection of total antioxidant capacity (TAC) of wine

The TAC of samples was measured with free radicals-scavenging activity assays (ABTS and DPPH), and ferric reducing-antioxidant power assay (FRAP). For all assays, results were obtained by interpolating the absorbance values on a calibration curve. All samples were analyzed in triplicate.

2.6.1. Free radicals-scavenging activity (ABTS)

100 μL of the appropriately diluted sample was mixed with 3 mL of ABTS (dissolved in methanol), and the absorbance was measured at 734 nm after a 4-min reaction.

2.6.2. Ferric reducing-antioxidant power (FRAP)

100 μL of appropriately diluted sample was added to 3 mL of the FRAP reagent (dissolved in methanol), and the absorbance was measured at 593 nm after incubating at room temperature for 6 min in the dark.

2.6.3. Free radicals-scavenging activity (DPPH)

100 μL of the appropriately diluted sample was added to 3 mL of 60 μM DPPH (dissolved in methanol), incubated for 15 min in the dark and measured at 515 nm.

2.7. Identification and extraction of anthocyanins compounds by UPLC-MS^E

For UPLC-MS^E analyses, grape pulp skin was vacuum freeze-dried. A ball mill was used to grind the sample (30 Hz, 1.5 min) to the powder. Fifty mg of the powder was weighed and dissolved in 500 μL of extraction solution (50 % methanol aqueous solution with 0.1 % hydrochloric acid). The mixture was stirred for 5 min, ultrasonic for 5 min, and centrifuged for 3 min (12, 000 r/min, 4 °C). The supernatant was then absorbed, and the operation was repeated once. The supernatant was combined, filtered through a microporous filter membrane (0.22 μm pore size), and stored in a sample vial for LC-MS/MS analysis.

The treatment of the wine sample involved thawing the plant material stored at ultra-low temperatures on ice. After vortex mixing, 50 μL was removed and dissolved in 950 μL extraction solution (50 % methanol aqueous solution with 0.1 % hydrochloric acid). The mixture was vortexed for 5 min, subjected to ultrasonic treatment for 5 min, and centrifuged for 3 min (12, 000 r/min, 4 °C), supernatant was absorbed, filtered through a microporous filter membrane (0.22 μm pore size), and stored in the sample bottle for LC-MS/MS analysis.

Data collection systems for the analysis and evaluation of anthocyanins mainly utilize Ultra Performance Liquid Chromatography (UPLC) (ExionLC™ AD, https://sciex.com.cn/) and Tandem Mass Spectrometry (MS/MS) (QTRAP® 6500+, https://sciex.com.cn/). Anthocyanins and anthocyanin-derived compounds were separated using an ACQUITY BEH C18 chromatographic column (1.7 μm, 2.1 mm × 100 mm). Mobile phase A consisted of ultra-pure water (0.1 % formic acid added), and the phase B was methanol (with 0.1 % formic acid added). The elution gradient started at 0.00 min with a B phase ratio of 5 %, increasing to 50 % at 6.00 min, to 95 % at 12.00 min, maintaining that ratio for 2 min, then decreasing to 5 % at 14 min, and equilibrating for 2 min. The flow rate was set at 0.35 mL/min. The column temperature was maintained at 40 °C. The sample volume used was 2 μL.

The mass spectrum conditions are as follows: Electrospray Ionization (ESI) temperature is 550 °C, mass spectrum voltage is 5500 V in positive ion mode, Curtain Gas (CUR) is 35 psi. In Q-Trap 6500+, each ion pair is scanned against an optimized Declustering Potential (DP) and Collision Energy (CE).

The qualitative and quantitative analysis relies on the Metware Database (MWDB), which is constructed from standard products, Qualitative analysis is conducted on the data obtained from mass spectrometry, while quantification is performed using Multiple Reaction Monitoring (MRM) analysis via triple quadrupole mass spectrometry. In the MRM model workflow: Screening: The first quadrupole screens the precursor ions (parent ions) of the target substances, excluding ions corresponding to other molecular weights to reduce interference. Fragmentation: After ionization in the collision chamber, the precursor ions fragment into several characteristic fragment ions. Filtering: The fragment ions are filtered through the second and third quadrupoles to select the desired characteristic fragment ions, further eliminating non-target ions. This enhances the accuracy and repeatability of quantification. After obtaining mass spectrometry data from various samples, the chromatographic peaks of all target compounds are integrated, and quantitative analysis is conducted using standard curves.

The results were evaluated as follows: Analyst 1.6.3 software was utilized for processing mass spectrum data. Multi Quant 3.0.3 software was used to Employed for further data analysis, referencing the retention time and peak type information of standard products. Integral correction is applied to the mass spectrum peaks detected across different samples to ensure qualitative and quantitative accuracy.

2.8. Identification and extraction of non-anthocyanin flavonoids compounds by UPLC-MS^E

After skinning the berries, grape skin samples were freeze-dried under vacuum, The dreid samples were then ground using a ball mill (30 Hz,1.5 min) to a powder form. 20 mg of powder was weighed, further adding 10 μL of internal standard mixed working solution with a concentration of 4000 nmol/L and 500 μL of 70 % methanol solution. Following ultrasonic treatment for 30 min. Centrifuge at 4 °C (rotation speed 12, 000 r/min, 5 min), extract the supernatant, filter the sample suing a 0.22 μm filter membrane, and store it in a sample vial for LC-MS/MS analysis.

The treatment of the wine sample is as follows: Thaw the ultra-low temperature preserved sample on ice. After vortex mixing, 50 μL sample was added 10 μL of internal standard mixed working solution with a concentration of 4000 nmol/L and 500 μL of 70 % methanol solution. After ultrasound for 30 min and centrifugation at 4 °C (rotation speed 12, 000 r/min, 5 min), the supernatant was absorbed, the sample was filtered by 0.22 μm filter membrane, and store in a sample vial for LC-MS/MS analysis.

The data acquisition system for analyzing and evaluating non-anthocyanin flavonoids primarily employs ultra-high performance liquid chromatography (UHPLC) and tandem mass spectrometry (MS/MS). The non-anthocyanin flavonoids were isolated using Waters ACQUITY UPLC HSS T3 C18 column (1.8 μm, 100 mm × 2.1 mm i.d.). The mobile phase A is ultra-pure water (0.05 % formic acid added), and the phase B is acetonitrile (0.05 % formic acid added). The flow rate was 0.35 mL/min. The column temperature was 40 °C. The sample volume was 2 μL. The elution gradient is set as 90:10 (*V*/V) for 0 min A/B, 80:20 (V/V) for 1 min A/B, 30:70 (V/V) for 9 min, 5:95 (V/V) for 12.5 min A/B, and 5:95 (V/V) for 13.5 min. The value is 90:10 (V/V) in 13.6 min and 90:10 (V/V) in 15 min. The mass spectrum conditions are as follows: electrospray ion source temperature of 550 °C, mass spectrum voltage of 5500 V in positive ion mode, mass spectrum voltage of −4500 V in

negative ion mode, and gas curtain gas of 35 psi. In Q-Trap 6500+, each ion pair is scanned according to the optimized de-clustering voltage and collision energy. Data collection and quantification for non-anthocyanin flavonoids follow the same protocols as those used for anthocyanins.

2.9. Statistical analysis

Data are expressed as mean ± standard deviation (SD). Analysis of variance (ANOVA) was performed for each variable to evaluate differences between cultivars and samples types. When significance was found ($p < 0.05$), further analysis was conducted. Orthogonal partial least squares discrimination analysis (OPLS-DA) was performed using SIMCA 14.1 software to detect clustering or separation between grape and wine samples. In all figures and tables, data are the mean ± standard deviation of three biological replicates. Different letters indicate significant differences among four cultivars or wines ($p < 0.05$).

3. Results and discussion

3.1. Meteorological characteristics

The meteorological data are presented in. Fig. 1 (A and B) illustrate the number of days in 2021 when the maximum temperature exceeded 40 °C across various regions of China, including Xinjiang. This data helps us assess the frequency of extreme high-temperature events during the specific period. A comparison reveals that Xinjiang, particularly the Turpan Basin, experienced significantly more high-temperature days than the national average. This highlights the region's vulnerability to extreme high-temperature conditions, especially in the context of its arid and semi-arid climate. Fig. 1C shows that summer temperatures in the Turpan Basin are extremely high, with average temperatures from June to August ranging from 24 °C to 36 °C. The number of days when the daily maximum temperature exceeds 35 °C can exceed 72 days, with

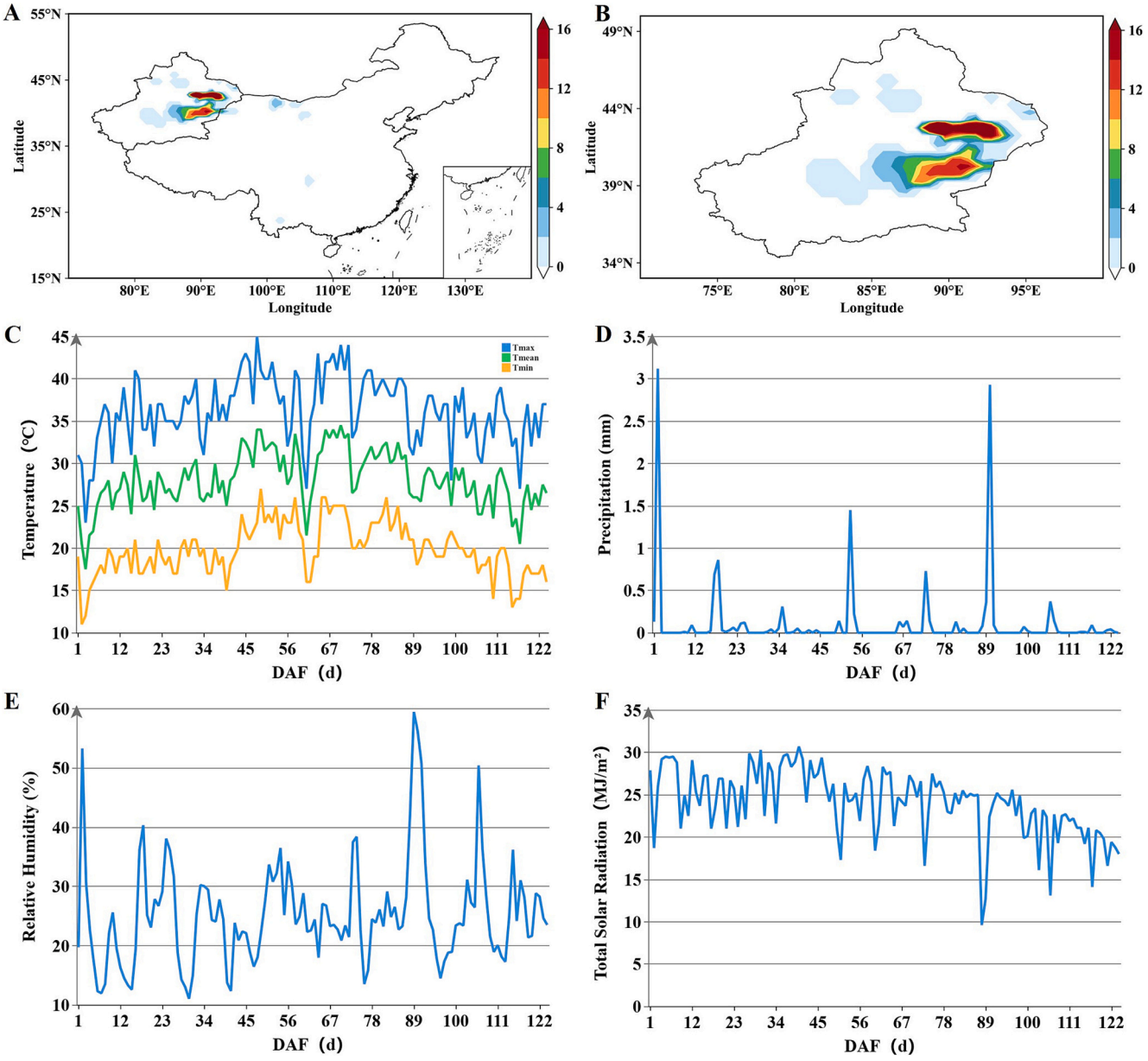

Fig. 1. Comprehensive analysis of climatic conditions and agricultural cycles in China and Xinjiang: (A) Geographical distribution of days exceeding 40 °C in China for 2021; (B) Geographical distribution of high-temperature days in Xinjiang for 2021; (C) Temperature data where Tmax indicates the daily maximum temperature, Tmean indicates the daily average temperature, Tmin indicates the daily minimum temperature; (D) Precipitation levels in the experimental vineyards from April to October; (E) Relative humidity, (F) Total solar radiation intensity. DAF indicates Days After Flowering.

July alone recording extreme temperatures above 40 °C for 19 days. This constantly high-temperature environment acts as a natural catalyst for accelerating sugar accumulation and enhancing flavor components in grape fruits (Lecourieux et al., 2017).

Conversely, the Turpan Basin is characterized by extremely low annual precipitation, averaging only 29.75 mm throughout the year, with most months recording precipitation well below the threshold of 5.31 mm (Fig. 1D). Meanwhile, the average relative humidity in the region fluctuates between 9.50 % and 63.00 %, remaining below 50 % most of the time (Fig. 1E). These extremely dry climate conditions undoubtedly intensify the water stress for grapevines.

It is worth noting that water stress is known to stimulate the accumulation of phenols in grapes, a physiological response that enhances antioxidant potential and overall wine quality (Lecourieux et al., 2017). Additionally, strong solar radiation (Fig. 1F) promotes photosynthesis in grapes, supporting sugar and flavor substance accumulation. The low relative humidity in Turpan helps control the pests and diseases in the vineyards, minimizing grape damage. However, elevated temperatures may also influence flavonol synthesis, potentially leading to a comprehensive decline in metabolic activity across the vine (Gouot, Smith, Holzapfel, Walker, & Barril, 2019).

3.2. Physical and chemical parameters of grapes and wine

Table S1 presents the physicochemical parameters of four wine grape cultivars—Cabernet Sauvignon, Marselan, Saperavi and Syrah, highlighting their performance differences in the extreme high-temperature environment of the Turpan Basin. The analysis revealed significant variations in single berry weight, soluble solids, titratable acidity, reducing sugar, sugar-acid ratio, and juice yield, providing insights into the mechanisms behind each cultivar's performance in heat and drought conditions. Among them, Saperavi exhibited the largest single berry weight (2.18 g), suggesting that its fruit was more fully developed, potentially indicating better adaption to extreme heat and drought conditions(Cola, Failla, Maghradze, Megrelidze, & Mariani, 2017). Marselan had the highest soluble solids content (26.23°Brix), which may correlate with a higher alcohol potential and the unique sugar accumulation mechanisms in Turpan's extreme climate. Saperavi showed the highest titrated acidity (0.80 %), indicating that wines from this cultivar may possess greater acidity and a pronounced structure. In terms of sugar-acid ratio, Cabernet Sauvignon had a significantly higher sugar-acid ratio (54.09) compared to other cultivars, suggesting it maintained high sweetness and lower acidity, resulting in a better flavor balance under high-temperature conditions(Li, Li, Guan, Li, & Tao, 2025). In contrast, Saperavir had the lowest sugar-to-acid ratio (31.71), indicating that its wines may exhibit strong acidity and a refreshing taste. This difference may stem from the distinct metabolic responses of each cultivar to heat stress and water management. Saperavi also had the highest juice yield (50.57 %), indicating its grapes provided more juice during winemaking, aligning with its larger berry size and good yield performance under drought conditions.

In the physicochemical parameters of wine, although the alcohol concentrations of the four cultivars are relatively similar, significant differences exist in key quality indicators such as acidity and reducing sugar. Cabernet Sauvignon had the highest total acidity (7.85 g/L), suggesting that its wines may have a pronounced structure and aging potential. Conversely, Marselan had the lowest total acidity, indicating it may produce softer wines suitable for early consumption. Saperavi wines featured the highest reducing sugar content, well-balanced by their acidity, which may contribute to a complex and layered palate. The differences in pH reflect the adaptive strategies of the cultivars in the extreme environment of Turpan. Cabernet Sauvignon and Marselan exhibited relatively low pH values, indicating higher acidity, while Saperavi had a higher pH (4.01), which may be linked to its enhanced buffering capacity and antioxidant properties.

3.3. Color attribute of four wines

Based on the absorption analysis of wine samples in the visible light range of 400–780 nm, absorbance values at wavelengths of 450, 520, 570, and 630 nm were extracted and corrected for a 1 cm optical path. In the CIELAB color space, color is defined using three orthogonal independent parameters: L*, a*, and b*. Here, L* represents brightness, a* denotes the red-green components, and b* indicates the yellow-blue components (Ju et al., 2021). By analyzing these color parameters along with chroma (C*ab), chroma angle (h*ab/°), and chromatic aberration measure (ΔEab) (Fig. 2), we can accurately characterize the color properties of wine. This analysis elucidates the effects of different grape cultivars and climatic conditions on the wine's hue.

L* values range from 0 to 100, with higher L* values indicating lighter colors . Our findings show that the L* values for Cabernet Sauvignon (77.53) and Marselan wine' (75.81) are higher than those for Syrah (72.41) and Saperavi (67.44) (Fig. 2). This difference may be attributed to the high-temperature environment of the Turpan Basin, which can lead to greater brightness due to lower concentrations of anthocyanins in the grape skins during ripening and/or a increased susceptibility to oxidation (Boulton, & j. o. e., & viticulture., 2001). Additionally, the brightness of wine correlates with antioxidant capacity; higher brightness typically signifies a lower flavonoid concentration, potentially affecting antioxidant properties.

The a* value reflects the red content of the wine. In this study, Saperavi wine exhibited a significantly higher a* value (30.34) compared to Cabernet Sauvignon (21.49), indicating a stronger red character in Saperavi. The low a* value observed in Syrah suggests it has relatively little red content, potentially appearing more purple or in other hues. This may be due to a higher concentration of flavonoids and anthocyanins in the skins of Saperavi grapes, enhanced by the Turpan Basin's high temperatures(R. Boulton, 2001).

The b* value indicates the yellow content of the wine. The Syrah had a lower b* value (6.82) than Cabernet Sauvignon (10.63), suggesting a higher blue component. This phenomenon may relate to the extreme climatic conditions in the Turpan Basin, where high temperatures could promote the formation of blue pigments. Some in - vitro experiments have shown that when grape cell cultures are exposed to high - temperature conditions, there is an increase in the production of delphinidin - based anthocyanins. These studies simulate the physiological

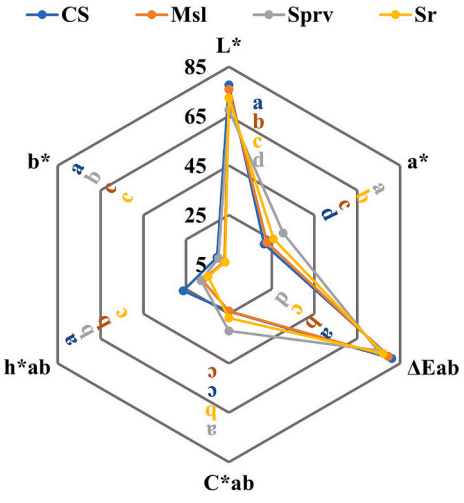

Fig. 2. Chroma CIELab representation. Abbreviation: L* (lightness), a* (green/red), b* (blue/yellow), C^*_{ab} (chroma), h^*_{ab} (hue angle), ΔEab (chromatic aberration measure). Data are illustrated in a radar chart as mean ± SD ($n = 3$). Different letters indicate a significant differences at each sampling point ($P < 0.05$). (For interpretation of the references to color in this figure legend, the reader is referred to the web version of this article.)

environment of grapevines under heat stress and provide direct evidence for the effect of high temperatures on the synthesis of blue - colored pigments. (Czibulya, Horváth, Kollár, Nikfardjam, & Kunsági-Máté, 2015; Medina-Plaza, Dubois, Tomasino, & Oberholster, 2024).

C*ab represents chroma, combining a* and b* values to reflect the saturation of the wine's color. Higher C*ab values indicate more concentrated and saturated colors (Sáenz Gamasa et al., 2009). Saperavi boasts the highest chroma (31.91), indicating stronger color saturation and a more vibrant visual impact. In contrast, Syrah has a lower chroma (26.68), resulting in a lighter appearance.

The chroma angle h*ab/ (°) denotes the overall tendency of a wine's color, positioning its hue within the color spectrum. Generally, the hue angle for red wine ranges from 0° and 90°. Small hue values suggest a tendency toward purple or ruby red, typical of fresh red wines. As the hue angle increases, the color gradually shifts toward tile red or brick red, often associated with the aging process. Cabernet Sauvignon (26.31) and Marselan (17.51) exhibit higher hue angles, indicating richer tonal characteristics, while Syrah (14.81) and Saperavi (18.03) show relatively lower tonal diversity.

The total color difference, ΔEab, incorporates contributions from L*, a*, and b* to indicate the human eye's ability to perceive color variations between samples. The color differences among the wine of four cultivars are visually apparent, with higher saturation of Cabernet Sauvignon (81.15) and Marselan (79.48) displaying more intense coloration, while Syrah (77.17) and Saperavi (74.61) appear less saturated and more muted. Jackson (Jackson, 2008) notes that color characteristics impact sensory quality and antioxidant properties, with flavonoid concentration influencing ΔEab values.

In summary, Cabernet Sauvignon and Marselan demonstrate superior performance in brightness, saturation, and tonal richness, showcasing bright and vibrant colors. In contrast, Syrah and Saperavi exhibit darker hues and may present a more muted and intense red tone. A deeper understanding of these color characteristics enhances our knowledge of the sensory properties and health benefits of wine, particularly for cultivars grown under extreme climatic conditions.

3.4. Anthocyanins profile in grape and wine samples

Anthocyanins are the primary phenolic compounds in grapes, with five main colored aglycons identified in *V. vinifera* L, namely cyanidin, peonidin, delphinidin, petunidin and malvidin (Abe, Da Mota, Lajolo, & Genovese, 2007). These compounds are found in the berry skin and are the key contributors to the red color of grapes and wines (Lingua, Fabani, Wunderlin, & Baroni, 2016). The results obtained for individual phenolic compounds identified in grape and wine samples from four cultivated grape cultivars are shown in Table 1. Overall, the analysis revealed that climate significantly influenced ($p < 0.05$) the content of certain individual polyphenols. A total of 36 anthocyanins and anthocyanin-derived compounds were identified in grape skins and 25 in wine, which included anthocyanins, glycoylated anthocyanins, acylated anthocyanins, pyranoid anthocyanins and polymerized anthocyanins. Anthocyanins and acylated anthocyanins, derived from the maceration process during winemaking, are crucial for determining the red color of young wines. Additionally, anthocyanins and polymerized anthocyanins can react with tannins or certain byproducts of yeast during fermentation, such as acetaldehyde, pyruvate, and vinylphenol, finally affecting their stability and color (Kumar, Tian, & Harrison, 2022).

Among the four grape cultivars, Saperavi exhibited the highest total anthocyanin concentration, with 11,680.975 mg/kg in grape skins and 178.875 mg/L in wine, followed by Syrah, with 5874.331 mg/kg in grape skins and 138.246 mg/L in wine. The concentration of total anthocyanins in Marselan and Cabernet Sauvignon was relatively low, at 5395.461 mg/kg and 5070.748 mg/kg in grape skins, and 110.240 mg/L and 112.001 mg/L in wine, respectively. These differences reflect varying efficiencies of anthocyanin retention among various cultivars during the winemaking, which are influenced by factors such as grape's genetic background, winemaking process, and its chemical composition. For example, the extraction and stability of anthocyanins can differ significantly between varieties, affecting their final concentration in wine. Factors such as temperature, pH, and yeast species also play critical roles in anthocyanin retention during the brewing process, thereby improving the color and quality of the wine.

In Saperavi, centaurin and its derivatives accounted for 82.29 % of the total anthocyanins in grape skins and 95.27 % in wine, contributing to the variety's dark and stable color. Syrah's anthocyanins and their derivatives represented 65.34 % in grape skins and 89.45 % in wine, which may enhance its antioxidant properties despite lower anthocyanin concentrations and higher flavonoid levels (He et al., 2012b). Significant differences were observed in the concentrations of melastanin (Petunidin), Delphinidin, and Peonidin among cultivars, all of which influence the color and flavor of wine (Castillo-Muñoz et al., 2007). The concentration of anthocyanins in grape skins and wine differed significantly between grape skins and wine, with transfer efficiencies varying by variety. Saperavi demonstrated the highest anthocyanin transfer efficiency during brewing, indicating strong anthocyanin retention capabilities during brewing (Cheynier et al., 2006). In contrast, Syrah exhibited lower transfer efficiency suggesting a need for optimization in the brewing process to enhance anthocyanin stability. In conclusion, the composition and concentration of anthocyanins in different grape cultivars significantly affect the color, aroma, and flavor characteristics of wine. Saperavi, with its high anthocyanin concentration and transfer efficiency, can produce wines with dark, stable coloration. On the other hand, while Syrah has lower anthocyanin levels, its richness in flavonoids may provide advantages in antioxidant properties and complex flavor profiles. Marselan and Cabernet Sauvignon, despite lower anthocyanin concentrations, demonstrate better color stability during brewing.

3.5. Non-anthocyanin flavonoids in grape berries and wine from four cultivers

Fifty-two non-anthocyanin flavonoids were identified and quantified in grape samples, while fifty-one were found in wine samples (Table 2). The primary compounds identified include well-known flavonoids structures commonly reported for *Vitis vinifera* L., such as kaempferol, myricetin, quercetin and isorhamnetin, along with their monoglycoside derivatives (Lingua et al., 2016). These flavonoids belong to various chemical classes, including flavonols, flavanols, catechins, chalcones, etc.. Remarkably, Myricitrin, a compound associated with anti-inflammatory activity, was also detected (Patel et al., 2016). The concentration of total flavonoids in grape skin was highest at 2334.702 mg/kg. Among the cultivars, Marselan has the lowest concentration (1110.089 mg/kg), followed by Cabernet Sauvignon (2145.634 mg/kg) and Saperavi (1626.978 mg/kg). In wine, total flavonoid concentrations are generally lower than in grape skins, with Syrah exhibiting the highest levels. This suggests that Syrah maintains better stability and transfer efficiency of flavonoids during the winemaking process (Wang, Race, Shrikhande, & Chemistry, 2003).

Syrah also had the highest flavonol concentration in grape skins, particularly quercetin-3-O-glucoside, which comprised over 70 % of the total flavonols, Cabernet Sauvignon followed, with baicalin accounting for about 65 % of its flavonol content. In wine, Cabernet Sauvignon retains these components effectively, enhancing its antioxidant properties (Hanlin et al., 2010). Meanwhile, Saperavi and Marselan had lower flavonol contents, at approximately 50 % and 45 % of their total flavonols, respectively, which may negatively affect the antioxidant capacity of their wines. Saperavi exhibited the highest total flavonoid concentration in grape skin, primarily composed of diosmin and narcissin, which accounted for over 40 % of the total flavonoids. Saperavi also performs well in the retention of flavonoids in wine, contributing significantly to the flavor profile of its wines (Mattivi et al., 2006). Syrah

Table 1
Anthocyanin phenolics in four cultivars of grape berries and wine from the Turpan Basin, Xinjiang.

NO.	Anthocyanin phenolics	Grape(mg/kg)				Wine(mg/L)			
		CS	Msl	Sprv	Sr	CS	Msl	Sprv	Sr
1	Malvidin-3-O-glucoside	3856.254 ± 44.987c	4290.806 ± 267.946bc	6690.056 ± 98.308a	3949.594 ± 18.901c	81.212 ± 3.083b	81.915 ± 3.400b	117.014 ± 6.958a	83.348 ± 2.964b
2	Malvidin-3-O-(6-O-p-coumaroyl)-glucoside	90.710 ± 0.171d	134.511 ± 1.802c	187.664 ± 1.157a	144.297 ± 4.188b	20.500 ± 1.307c	21.853 ± 1.677bc	26.911 ± 2.688b	42.510 ± 2.383a
3	Malvidin-3,5-O-diglucoside	10.477 ± 0.018b	8.855 ± 0.373c	23.385 ± 0.533a	1.812 ± 0.018d	1.059 ± 0.040b	0.906 ± 0.007c	4.039 ± 0.084a	0.166 ± 0.007d
4	Malvidin-3-O-(6-O-malonyl-beta-D-glucoside)	7.441 ± 0.064b	8.072 ± 0.067a	5.528 ± 0.179c	3.380 ± 0.077d	0.048 ± 0.001a	0.035 ± 0.001b	0.038 ± 0.004b	0.026 ± 0.005c
5	Malvidin-3-O-(6″-acetylglucoside)-5-glucoside	2.645 ± 0.038a	0.905 ± 0.019bc	1.044 ± 0.008b	1.172 ± 0.151b	0.286 ± 0.008a	0.286 ± 0.008a	0.271 ± 0.012ab	0.254 ± 0.006b
6	Malvidin-3-O-arabinoside	0.944 ± 0.007c	1.173 ± 0.020b	1.558 ± 0.029a	1.128 ± 0.021b	0.012 ± 0.000b	0.010 ± 0.001c	0.010 ± 0.000c	0.014 ± 0.001a
7	Malvidin-3-O-5-O-(6-O-coumaroyl)-diglucoside	0.240 ± 0.020d	0.484 ± 0.008b	1.401 ± 0.018a	0.358 ± 0.004c	0.010 ± 0.000c	0.019 ± 0.000ab	0.018 ± 0.001b	0.022 ± 0.002a
	Malvidin	3968.71 ± 45.2c	4441.81 ± 265.9b	6910.64 ± 99.99a	4101.74 ± 23.16c	103.13 ± 4.27c	105.03 ± 5.07c	148.3 ± 9.56a	126.34 ± 5.36b
8	Petunidin-3-O-glucoside	423.138 ± 2.625c	418.129 ± 6.733c	1934.329 ± 21.698a	678.162 ± 10.024b	4.361 ± 0.127b	2.955 ± 0.059c	13.458 ± 0.762a	5.383 ± 0.336b
9	Petunidin-3-O-galactoside	52.410 ± 0.695c	52.164 ± 1.956c	247.663 ± 1.966a	85.426 ± 1.037b	nd	nd	nd	nd
10	Petunidin-3-O-arabinoside	0.336 ± 0.007c	0.303 ± 0.008d	0.794 ± 0.008a	0.490 ± 0.009b	nd	nd	nd	nd
11	Petunidin-3-O-sophoroside	0.258 ± 0.001c	0.226 ± 0.015c	0.950 ± .044a	0.450 ± 0.011b	nd	nd	nd	nd
12	Petunidin-3-O-(6-O-p-coumaroyl)-glucoside	nd	nd	nd	nd	0.004 ± 0.001d	0.006 ± 0.000c	0.019 ± 0.001b	0.022 ± 0.001a
13	Petunidin-3-O-5-O-(6-O-coumaroyl)-diglucoside	nd	nd	nd	nd	nd	nd	0.053 ± 0.005a	nd
	Petunidin	476.14 ± 2.22c	470.82 ± 8.63c	2183.74 ± 23.44a	764.53 ± 8.99b	4.36 ± 0.13c	2.96 ± 0.06d	13.53 ± 0.76a	5.41 ± 0.34b
14	Delphinidin-3-O-glucoside	373.795 ± 7.527c	299.586 ± 6.799d	1711.477 ± 13.536a	445.348 ± 21.781b	2.543 ± 0.013b	1.120 ± 0.107d	8.457 ± 0.082a	2.164 ± 0.123c
15	Delphinidin-3-O-(6-O-p-coumaroyl)-glucoside	5.689 ± 0.062c	3.652 ± 0.046d	27.382 ± 0.338a	18.978 ± 0.366b	nd	nd	nd	nd
16	Delphinidin-3-O-arabinoside	0.114 ± 0.005c	0.101 ± 0.001c	0.215 ± 0.007a	0.135 ± 0.007b	nd	nd	nd	nd
17	Delphinidin-3-O-sambubioside	0.111 ± 0.002b	0.225 ± 0.008a	0.066 ± 0.001c	nd	nd	nd	nd	nd
18	Delphinidin-3-O-rutinoside-5-O-glucoside	0.011 ± 0.001a	nd	nd	nd	nd	nd	nd	nd
19	Delphinidin-3-O-rutinoside	nd	0.018 ± 0.001a	nd	nd	nd	nd	nd	nd
20	Delphinidin-3-O-sophoroside	nd	nd	nd	nd	0.151 ± 0.002b	0.102 ± 0.001c	0.529 ± 0.027a	0.145 ± 0.008b
21	Delphinidin-3,5-O- glucoside	nd	nd	nd	nd	0.028 ± 0.001b	0.012 ± 0.001c	0.098 ± 0.005a	0.090 ± 0.001d
22	Delphinidin-3,5-O-diglucoside	nd	nd	nd	nd	nd	nd	0.807 ± 0.023a	nd
	Delphinidin	379.65 ± 7.6c	303.58 ± 6.85d	1739.41 ± 13.21a	464.46 ± 21.42b	2.72 ± 0.01b	1.23 ± 0.11d	9.89 ± 0.08a	2.4 ± 0.13c
23	Peonidin-3-O-glucoside	164.623 ± 2.126c	126.628 ± 1.178d	573.046 ± 5.414a	309.449 ± 3.128b	1.306 ± 0.021c	0.761 ± 0.059d	3.811 ± 0.194a	3.247 ± 0.189b
24	Peonidin-3-O-(6-O-p-coumaroyl)-glucoside	38.416 ± 0.364b	17.983 ± 0.876d	32.661 ± 0.574c	89.589 ± 0.576a	0.073 ± 0.001b	0.040 ± 0.001c	0.086 ± 0.005b	0.263 ± 0.018a
25	Peonidin-3,5-O-diglucoside	1.672 ± 0.057b	0.770 ± 0.014c	3.818 ± 0.212a	0.808 ± 0.013c	0.185 ± 0.006b	0.11 ± 0.003c	0.571 ± 0.024a	0.056 ± 0.006d
26	Peonidin-3-O-rutinoside	0.943 ± 0.012a	0.964 ± 0.007a	nd	nd	0.023 ± 0.001a	0.009 ± 0.001a	0.120 ± 0.155a	nd
27	Peonidin-3-O-(6-O-malonyl-beta-D-glucoside)	0.214 ± 0.010b	0.169 ± 0.004c	0.306 ± 0.006a	0.230 ± 0.018b	nd	nd	nd	nd
28	Peonidin-3-O-arabinoside	0.015 ± 0.002b	0.015 ± 0.001b	0.018 ± 0.000b	0.040 ± 0.001a	nd	nd	nd	nd
29	Peonidin-3-O-5-O-(6-O-coumaroyl)-diglucoside	nd	nd	nd	nd	nd	nd	0.003 ± 0.001a	0.004 ± 0.001a
	Peonidin	205.88 ± 2.43c	146.53 ± 2.08d	609.85 ± 6.09a	400.12 ± 3.66b	1.59 ± 0.03c	0.93 ± 0.06d	4.59 ± 0.36a	3.57 ± 0.21b
30	Cyanidin-3-O-glucoside	22.253 ± 2.049c	13.108 ± 0.109 d	109.461 ± 2.803a	39.003 ± 0.896b	0.121 ± 0.002c	0.044 ± 0.001d	0.343 ± 0.012a	0.207 ± 0.007b
31	Cyanidin-3-O-(6-O-p-coumaroyl)-glucoside	16.398 ± 1.171c	17.709 ± 0.630c	110.437 ± 1.949a	101.085 ± 1.402b	0.052 ± 0.001a	0.029 ± 0.002a	0.135 ± 0.007a	0.303 ± 0.008a
32	Cyanidin-3-O-xyloside	0.144 ± 0.009d	0.186 ± 0.003c	0.846 ± 0.008a	0.224 ± 0.011b	nd	nd	nd	nd
33	Cyanidin-3-O-rutinoside	nd	0.091 ± 0.002a	nd	nd	nd	nd	nd	nd

(*continued on next page*)

Table 1 (*continued*)

NO.	Anthocyanin phenolics	Grape(mg/kg)				Wine(mg/L)			
		CS	Msl	Sprv	Sr	CS	Msl	Sprv	Sr
34	Cyanidin-3-O-galactoside	0.312 ± 0.011a	0.164 ± 0.006b	nd	nd	nd	nd	nd	nd
35	Cyanidin-3-O-sambubioside	0.003 ± 0.001a	nd	nd	nd	nd	nd	nd	nd
36	Cyanidin-3-O-sambubioside-5-O-glucoside	0.010 ± 0.001a	nd	nd	nd	nd	nd	nd	nd
37	Cyanidin-3-O-sophoroside	nd	nd	0.031 ± 0.002a	0.021 ± 0.001b	0.002 ± 0.000b	nd	0.011 ± 0.001a	0.002 ± 0.001b
38	Cyanidin-3-O-arabinoside	nd	nd	0.010 ± 0.001a	nd	nd	nd	nd	nd
39	Cyanidin-3,5-O-diglucoside	nd	0.062 ± 0.001c	0.165 ± 0.002a	0.107 ± 0.006b	0.023 ± 0.001b	0.013 ± 0.001c	0.055 ± 0.005a	0.011 ± 0.001c
40	Cyanidin-3-(6-O-p-caffeoyl)-glucoside	nd	nd	nd	nd	0.000 ± 0.000c	nd	0.005 ± 0.000a	0.003 ± 0.001b
	Cyanidin	39.11 ± 3.2c	31.32 ± 0.55d	220.96 ± 4.73a	140.78 ± 0.32b	0.2 ± 0c	0.09 ± 0d	0.55 ± 0.01a	0.53 ± 0.02b
41	Pelargonidin-3-O-glucoside	1.211 ± 0.010c	1.373 ± 0.045c	16.252 ± 0.220a	0.139 ± 0.180b	0.004 ± 0.001c	0.002 ± 0.000d	0.018 ± 0.001a	0.008 ± 0.001b
42	Pelargonidin-3-O-(6-O-p-coumaroyl)-glucoside	0.046 ± 0.002a	0.028 ± 0.001b	nd	nd	nd	nd	nd	nd
43	Pelargonidin-3,5-O-diglucoside	nd	nd	0.138 ± 0.180a	nd	nd	nd	nd	nd
	Pelargonidin	1.26 ± 0.01c	1.4 ± 0.05c	16.39 ± 0.35a	2.71 ± 0.01b	0 ± 0c	0 ± 0d	0.02 ± 0a	0.01 ± 0b
	Total content	5070.75 ± 60.5d	5395.46 ± 249.97c	11,680.97 ± 119.38a	5874.33 ± 14.27b	112 ± 4.13c	110.24 ± 5.17c	176.88 ± 10.69a	138.25 ± 5.98b

nd: not detected. Data are the mean ± standard deviation of three biological replicates. Different letters indicate significant differences among four cultivars or wines ($p < 0.05$).

showed notable level of flavanonols and chalcones, with each presenting 10 %–15 % of the total flavones content. These components are better retained in wine, contributing to Syrah's unique flavor and high antioxidant properties. Overall, significant differences exist in the accumulation and retention of flavonoids among the different grape cultivars. Syrah demonstrates superior performance in flavonols, flavonoids, and flavanols, indicating its advantages in the accumulation and transfer efficiency of these compounds. This makes Syrah particularly suitable for producing wines with high antioxidant properties.

3.6. Total antioxidant capacity in vitro of four cultivars of wine

Free radical-scavenging assays are crucial for assessing an antioxidant's ability to protect biological and food systems from reactive radical species that can damage lipoproteins, polyunsaturated fatty acids, DNA, and proteins. The antioxidant capacity varies across grape cultivars and their wines, making it essential to employ multiple methods to capture the different action mechanisms of antioxidants. The ABTS test focuses on electron transfer, measuring the ability of antioxidants to eliminate ABTS radicals. In contrast, the DPPH test evaluates how antioxidants neutralize stable DPPH radicals through either electron transfer or hydrogen atom transfer, providing direct insight into a wine's radical-scavenging properties. Meanwhile, the FRAP test assesses the reductive potential by measuring a wine's ability to reduce iron ions to ferrous ions, highlighting its electron transfer capabilities. Given the distinct focus of each method, a comprehensive evaluation of antioxidant activity requires the use of multiple tests (Re et al., 1999).

The antioxidant results are illustrated in Fig. 3. In the ABTS assay, Cabernet Sauvignon exhibited the highest antioxidant activity at 4777.5 mg TE/mL, significantly surpassing Syrah, Saperavi, and Marselan. This underscores Cabernet Sauvignon's robust capacity to neutralize ABTS free radicals.

Additionally, in the FRAP assay, Cabernet Sauvignon also demonstrated superior reduction potential, achieving 1394 μmol/g. This highlights its potent ability to reduce iron ions, thereby enhancing its role in electron transfer and metal chelation—key mechanisms in oxidative defense.

The DPPH assay revealed that Saperavi and Marselan had the highest free radical scavenging abilities at 27.25 mg TE/mL and 27.23 mg TE/mL, respectively; these values were marginally higher than those of Cabernet Sauvignon (27.08 mg TE/mL) and Syrah (26.73 mg TE/mL). Despite their lower performance in the ABTS and FRAP assays, Saperavi and Marselan exhibited distinct advantages in free radical scavenging (Ieri et al., 2021).

These findings elucidate the variations in antioxidant capacities among grape cultivars. The exceptional performance of Cabernet Sauvignon in both the ABTS and FRAP assays indicates its effectiveness in delaying oxidation processes, thus preserving wine stability and extending shelf life. The antioxidant properties inherent to this variety are crucial for preventing oxidation-induced color changes, flavor degradation, and nutrient loss during storage (Halliwell & r., 2012), making it a preferred choice for high-quality wine production.

Conversely, although Saperavi and Marselan received modest scores on the ABTS and FRAP tests, they excelled in scavenging free radicals, suggesting potential health benefits by mitigating excess free radicals that can lead to oxidative stress associated with aging and chronic diseases. Lastly, Syrah displayed consistent performance across all assays, indicating a balanced antioxidant profile that may contribute to flavor stability alongside combined antioxidant efficacy (Savalekar et al., 2019).

3.7. Multivariate statistical analysis of flavonoid compounds in grapes and wines

Stoichiometric approaches, particularly principal component analysis (PCA) and orthogonal partial least squares discriminant analysis (OPLS-DA), were employed to investigated the distribution and significance of phenolic components across diverse grape cultivars and their corresponding wine samples (Fig. 4.). Following data rectification, PCA was conducted for each grape variety and wine sample, allowing us to project and compare all extracts in this study. The multivariate analysis from the relative ion abundance of each compound allowed us to project and compared all the extracts in this present study. The PCA loadings biplot in Fig. 4**.** Facilitates the assessment of multivariate variations, elucidating overall differences between the samples (Santos et al., 2019). Notably, the grape samples from Saperavi and wine samples from

Table 2
Non-anthocyanin flavonoids in grape and wine samples of four cultivars from the Turpan Basin, Xinjiang.

NO.	Non-anthocyanin flavonoids	Grape (mg/kg)				Wine (mg/L)			
		CS	Msl	Sprv	Sr	CS	Msl	Sprv	Sr
1	Naringenin chalcone	0.563 ± 0.039a	0.469 ± 0.026a	0.668 ± 0.080a	0.514 ± 0.117a	0.569 ± 0.101a	0.573 ± 0.064a	0.426 ± 0.071a	0.468 ± 0.083a
2	Phloretin	0.039 ± 0.006c	0.034 ± 0.001c	0.099 ± 0.009a	0.062 ± 0.007b	0.024 ± 0.005b	0.204 ± 0.018a	0.017 ± 0.003b	0.024 ± 0.008b
3	Phlorizin	1.889 ± 0.264c	9.842 ± 2.037b	8.020 ± 0.280b	14.155 ± 1.449a	2.193 ± 0.180b	1.135 ± 0.098c	2.263 ± 0.111b	2.707 ± 0.168a
4	Trilobatin	0.121 ± 0.018b	0.227 ± 0.069ab	0.357 ± 0.068a	0.270 ± 0.034a	nd	nd	nd	nd
5	Xanthohumol	nd	nd	nd	nd	nd	nd	0.002 ± 0.001a	nd
	Chalcones	2.61 ± 0.25c	10.58 ± 2.29b	9.14 ± 0.31b	15 ± 1.54a	2.79 ± 0.28b	1.91 ± 0.18c	2.71 ± 0.04b	3.2 ± 0.11a
6	(−)-Catechin	6.014 ± 1.547b	4.971 ± 1.406b	16.055 ± 2.248a	22.994 ± 5.204a	142.700 ± 13.928a	142.365 ± 13.844a	120.215 ± 16.441a	135.060 ± 14.354a
7	(−)-Catechin gallate	1.288 ± 0.295c	1.765 ± 0.390	22.375 ± 1.607a	3.971 ± 0.483b	0.667 ± 0.049b	0.725 ± 0.522b	0.188 ± 0.031b	2.205 ± 0.670a
8	(−)-Epicatechin	11.887 ± 1.058c	11.147 ± 1.175c	24.253 ± 4.983ab	44.708 ± 14.865a	145.786 ± 16.318ab	113.440 ± 11.467b	124.476 ± 10.605ab	148.263 ± 11.901a
9	(−)-Epigallocatechin	11.023 ± 1.937c	23.309 ± 3.772b	11.112 ± 1.334c	37.689 ± 5.972a	28.037 ± 1.102b	7.396 ± 0.432d	32.484 ± 2.449a	12.063 ± 1.301c
10	(−)-Gallocatechin	14.790 ± 1.671b	10.000 ± 1.874b	42.308 ± 6.659a	16.038 ± 3.115b	21.319 ± 1.068a	5.036 ± 0.393c	18.428 ± 1.739b	4.922 ± 0.081c
11	(−)-Gallocatechin gallate	0.954 ± 0.338c	1.924 ± 0.157bc	20.316 ± 7.052a	1.991 ± 0.605bc	0.345 ± 0.037a	0.285 ± 0.041ab	0.193 ± 0.009b	0.330 ± 0081a
12	Afzelechin	nd	nd	nd	nd	0.066 ± 0.008ab	0.096 ± 0.019a	0.047 ± 0.008bc	0.026 ± 0.008c
	Flavanols	45.96 ± 5.32b	53.12 ± 8.32b	136.42 ± 15.43a	127.39 ± 29.02a	338.92 ± 32.28a	269.34 ± 25.59b	296.03 ± 10.2b	302.87 ± 4.15ab
13	Eriodictyol	0.128 ± 0.017c	0.138 ± 0.021c	0.447 ± 0.024a	0.329 ± 0.059b	0.711 ± 0.016a	0.472 ± 0.042bc	0.536 ± 0.048b	0.427 ± 0.025c
14	Naringenin-7-glucoside	4.438 ± 0.033a	1.574 ± 0.112c	4.252 ± 0.723a	2.795 ± 0.580bc	nd	nd	nd	nd
15	Pinocembrin	0.018 ± 0.006b	0.088 ± 0.012a	0.034 ± 0.007b	0.022 ± 0.002b	0.029 ± 0.005a	0.042 ± 0.008a	0.028 ± 0.005a	0.029 ± 0.010a
16	Hesperetin	nd	nd	nd	nd	nd	0.001 ± 0.001a	nd	nd
17	Hesperidin	nd	nd	nd	nd	nd	nd	0.102 ± 0.020a	0097 ± 0.028a
18	Liquiritigenin	nd	nd	nd	nd	0.003 ± 0.001a	0.001 ± 0.001a	0.002 ± .001a	0.003 ± .002a
19	Narirutin	nd	nd	nd	nd	0.006 ± 0.001a	0.006 ± 0.001a	0.008 ± 0.003a	0.004 ± 0.001a
	Flavanones	4.58 ± 0.03a	1.8 ± 0.1c	4.73 ± 0.73a	3.15 ± 0.56b	0.75 ± 0.02a	0.52 ± 0.05b	0.68 ± 0.08a	0.56 ± 0.01b
20	Astilbin	68.371 ± 4.178a	23.261 ± 2.990b	2.284 ± 0.526c	63.535 ± 12.939a	6.858 ± 0.546b	6.487 ± 0.543b	3.549 ± 0.147c	9.270 ± 0.494a
21	Dihydrokaempferol	nd	nd	nd	0.693 ± 0.000	0.753 ± 0.047bc	1.174 ± 0.136a	0.588 ± 0.044c	0.787 ± 0.033bc
22	Dihydromyricetin	3.347 ± 0.416b	2.816 ± 0.573b	3.666 ± 0.190b	6.117 ± 0.361a	2.664 ± 0.1 ± 56b	3.034 ± 0.178ab	2.621 ± 0.195b	3.544 ± 0.467a
23	Engeletin	17.738 ± 3.050a	3.589 ± 0.713c	0.859 ± 0.160c	11.323 ± 1.662b	1.457 ± 0.144a	0.391 ± 0.035a	0.850 ± 0.073b	1.487 ± 0.061a
24	Isosilybin	nd	nd	nd	0.035 ± 0.001a	nd	nd	nd	nd
25	Silibinin	0.243 ± 0.041b	0.400 ± 0.066a	0.335 ± 0.070ab	0.183 ± 0.038b	0.007 ± 0.000b	0.029 ± 0.004a	0.036 ± 0.0.007a	0.038 ± 0.011a
26	Taxifolin	nd	nd	nd	1.471 ± 0.000a	2.891 ± 0.101ab	3.446 ± 0.388a	1.942 ± 0.082b	3.106 ± 0.099a
	Flavanonols	89.7 ± 3.3a	30.07 ± 3.37b	7.14 ± 0.86c	81.85 ± 15.04a	14.63 ± 0.97b	15.56 ± 1.26b	9.59 ± 0.54c	18.23 ± 0.71a
27	Diosmetin	nd	nd	nd	nd	0.001 ± 0.001a	0.001 ± 0.001a	0.002 ± 0.001a	0.001 ± 0.001a
28	5,7-Dihydroxy-3′,4′,5′-trimethoxyflavone	nd	nd	nd	nd	nd	nd	nd	nd
29	5-*O*-Demethylnobiletin	0.005 ± 0.005a	0.012 ± 0.012a	0.007 ± 0.008a	0.006 ± 0.003a	nd	nd	nd	nd
30	Apigenin 7-glucoside	0.051 ± 0.002a	0.026 ± 0.011b	0.026 ± 0.006a	0.047 ± 0.009a	nd	nd	nd	nd
31	Chrysin	nd	0.009 ± 0.003a	0.010 ± 0.003a	nd	nd	nd	nd	nd
32	Cynaroside	0.542 ± 0.053c	1.289 ± 0.091b	2.742 ± 0.066a	1.048 ± 0.502bc	nd	nd	nd	nd
33	Diosmin	52.348 ± 1.842c	42.035 ± 5.633c	142.638 ± 3.319b	218.571 ± 29.915a	0.730 ± 0.038c	0.351 ± 0.042d	2.070 ± 0.126b	3.097 ± 0.105

(*continued on next page*)

Table 2 (*continued*)

NO.	Non-anthocyanin flavonoids	Grape (mg/kg)				Wine (mg/L)			
		CS	Msl	Sprv	Sr	CS	Msl	Sprv	Sr
34	Limocitrin	28.606 ± 2.564a	25.261 ± 0.343ab	15.513 ± 0.497	20.229 ± 3.143b	nd	0.157 ± 0.011b	0.421 ± 0.051a	0.342 ± 0.040a
35	Luteolin	0.016 ± 0.012b	0.012 ± 0.008b	0.041 ± 0.005a	0.023 ± 0.003ab	0.005 ± 0.001a	nd	0.002 ± 0.001b	0.001 ± 0.001c
36	Narcissin	19.590 ± 0.730c	36.762 ± 3.007c	186.660 ± 3.958a	103.957 ± 17.17b	0.558 ± 0.056	0.445 ± 0029c	1.094 ± 0.110a	0.629 ± 0.030b
37	Nicotiflorin	3.759 ± 0.234b	2.262 ± 0.478b	21.519 ± 2.945a	26.776 ± 9.873a	0.175 ± 0.014c	0.276 ± 0.056b	0.465 ± 0.041a	0.193 ± 0.023bc
38	Tangeretin	0.002 ± 0.000a	0.002 ± 0.000a	0.002 ± 0.000a	0.002 ± 0.000a	nd	nd	nd	nd
39	Tricetin	0.263 ± 0.060b	0.100 ± 0.008b	1.315 ± 0.084a	0.258 ± 0.136b	nd	nd	nd	nd
40	Tricin	0.726 ± 0.280c	1.595 ± 0.462bc	4.775 ± 1.008a	2.357 ± 0.507bc	nd	nd	nd	nd
41	Homoplantaginin	nd	nd	nd	nd	0.004 ± 0.001b	nd	0.008 ± 0.001a	0.005 ± 0.001b
42	Jaceosidin	nd	nd	nd	nd	0.001 ± 0.001a	0.004 ± 0.001a	0.002 ± 0.001a	0.002 ± 0.001a
43	Pedalitin	nd	nd	nd	nd	nd	nd	0.007 ± 0.003a	0.007 ± 0.001a
44	Sakuranetin	nd	nd	nd	nd	0.001 ± 0.001a	nd	0.002 ± 0.002	nd
	Flavones	105.91 ± 1.7b	109.37 ± 9.77b	375.25 ± 3.4a	373.27 ± 60.8a	1.48 ± 0.11b	1.23 ± 0.14b	4.07 ± 0.33a	4.28 ± 0.09a
45	Afzelin	0.166 ± 0.087a	0.019 ± 0.009b	nd	0.066 ± 0.031ab	0.008 ± 0.001a	0.005 ± 0.003a	0.007 ± 0.002a	0.006 ± 0.003a
46	Astragalin	94.072 ± 26.841a	2.829 ± 0.591c	2.026 ± 1.296c	41.387 ± 21.285bc	3.062 ± 0.068ab	1.764 ± 0.172c	3.276 ± 0.283ab	3.625 ± 0.547a
47	Avicularin	12.067 ± 2.991a	0.722 ± 0.021b	0.242 ± 0.128b	8.604 ± 4.817a	0.137 ± 0.013a	0.071 ± 0.011b	0.143 ± 0.042a	0.170 ± 0.013a
48	Baimaside	7.702 ± 0.702c	5.289 ± 0.845c	33.834 ± 0.738a	13.583 ± 3.045b	0.537 ± 0.021c	0.475 ± 0.025c	0.752 ± 0.132b	0.321 ± 0.066a
49	Hyperoside	287.779 ± 31.858a	70.271 ± 17.520b	63.464 ± 3.364b	155.866 ± 63.97b	6.369 ± 0.394b	5.102 ± 0.108b	6.418 ± 0.485b	10.496 ± 1.528a
50	Isorhamnetin	0.343 ± 0.070ab	0.070 ± 0.005b	0.333 ± 0.012ab	1.474 ± 0.964a	0.029 ± 0.005a	0.004 ± 0.001c	0.016 ± 0.004b	0.017 ± 0.002b
51	Isorhamnetin 3-O-glucoside	149.358 ± 27.508ab	18.092 ± 3.558b	10.273 ± 2.156b	317.27 ± 138.32b	3.193 ± 0.182b	2.695 ± 0.137b	3.349 ± 0.278b	18.377 ± 1.176a
52	Isorhamnetin-3-O-neohespeidoside	19.908 ± 0.159c	43.708 ± 2.870c	218.317 ± 6.966a	131.195 ± 23.27b	0.285 ± 0.038b	0.253 ± 0.060b	0.791 ± 0.072a	0.697 ± 0.113a
53	Kaempferol	0.172 ± 0.075a	nd	nd	0.167 ± 0.036a	nd	nd	nd	nd
54	Laricitrin	0.915 ± 0.189ab	0.329 ± 0.031b	2.172 ± 0.118a	1.856 ± 0.161ab	0.047 ± 0.008a	0.021 ± 0.007a	0.044 ± 0.019a	0.029 ± 0.008a
55	Miquelianin	1198.801 ± 26.126a	690.558 ± 25.052bc	328.468 ± 56.951c	827.84 ± 269.22b	22.848 ± 2.657a	16.321 ± 1.670b	21.445 ± 1.745a	25.482 ± 2.630a
56	Myricetin	28.121 ± 7.823bc	5.989 ± 1.831c	138.064 ± 22.967a	35.368 ± 14.661bc	0.327 ± 0.035a	nd	0.263 ± 0.038a	nd
57	Myricitrin	0.671 ± 0.091b	0.554 ± 0.110b	1.294 ± 0.250a	0.715 ± 0.328b	0.055 ± 0.01b	0.190 ± 0.032a	0.055 ± 0.007b	0.144 ± 0.011a
58	Quercetin	0.905 ± 0.276a	0.108 ± 0.010a	0.237 ± 0.043a	1.862 ± 1.424a	0.149 ± 0.025a	0.009 ± 0.002c	0.098 ± 0.013b	0.031 ± 0.002c
59	Quercimeritrin	10.766 ± 2.231a	nd	nd	18.044 ± 8.126a	0.344 ± 0.051b	0.247 ± 0.028b	0.324 ± 0.029b	0.856 ± 0.049a
60	Quercitrin	12.452 ± 2.639a	3.029 ± 1.291b	0.320 ± 0.134	8.885 ± 3.035a	0.644 ± 0.022a	0.469 ± 0.049b	0.325 ± 0.036c	0.516 ± 0.019b
61	Rutin	71.395 ± 2.637c	60.184 ± 7.921c	298.399 ± 8.353a	169.421 ± 4.266b	1.863 ± 0.123b	2.622 ± 0.210a	2.561 ± 0.363a	0.957 ± 0.090c
62	Tiliroside	0.033 ± 0.000a	nd	nd	0.098 ± 0.047a	nd	nd	nd	nd
	Flavonols	1895.55 ± 85a	901.75 ± 57.96b	1097.44 ± 64.01b	1733.65 ± 504.81a	39.9 ± 3.56b	30.25 ± 2.5c	39.87 ± 3.29b	62.72 ± 5.69a
63	Genistin	0.413 ± 0.062a	0.499 ± 0.122a	nd	0.390 ± 0.126a	nd	nd	nd	nd
64	Glycitin	0.913 ± 0.237a	nd	nd	nd	nd	nd	nd	nd
65	Daidzein	nd	nd	nd	nd	nd	nd	0.008 ± 0.002a	nd
66	Puerarin	nd	nd	nd	nd	0.004 ± 0.001ab	0.005 ± 0.001a	0.004 ± 0.001ab	0.002 ± 0.001b
	Isoflavanones	1.33 ± 0.18a	0.5 ± 0.12b	0 ± 0c	0.39 ± 0.13b	0 ± 0b	0 ± 0b	0.01 ± 0a	0 ± 0b
	Total content	2145.63 ± 85.94a	1107.17 ± 69.93c	1630.13 ± 50.32b	2334.7 ± 409.37a	398.46 ± 37.05a	318.82 ± 29.68b	352.95 ± 14.47ab	391.86 ± 10.22a

nd: not detected. Data are the mean ± standard deviation of three biological replicates. Different letters indicate significant differences among four cultivars or wines ($p < 0.05$).

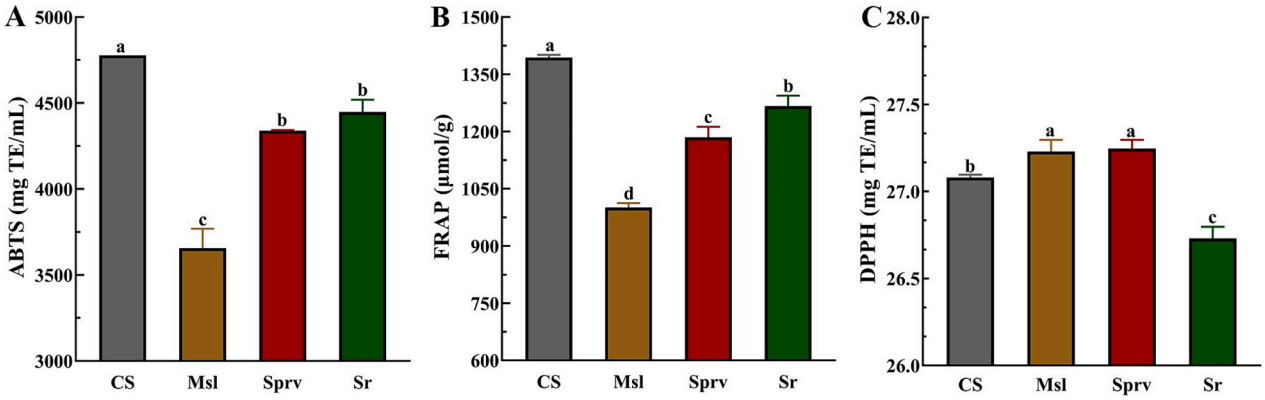

Fig. 3. Antioxidant capacity: (A) ABTS, (B) FRAP, (C) DPPH. Data are the mean ± standard deviation of three biological replicates. Different letters indicate significant differences among four cultivars or wines ($p < 0.05$).

Syrah are distinctly distinguishable from other samples along Principal Component 1 (PC1), which accounts for 83 % of the variance in grape samples and 49.4 % in wine samples. This differentiation is largely attributed to the identified anthocyanin phenolics, particularly the profile and relative abundance of Malvidin-3-O-glucoside.

In addition, the R^2X and Q^2 of the PCA model of grape samples both exceeded 0.9, indicating a robust model capable of effectively accounting for sample variability. For wine samples, both R^2X and Q^2 values surpassed 0.8, further affirming the model's reliability. PC1 and PC2 in Fig. 4A together accounted for 93.8 % of the variation in grape samples, while in Fig. 4D, they explained 49.4 % and 25 % of the variation in wine samples, respectively, highlighting significant disparities among different cultivars. PCA effectively discriminated samples of each variety, laying a critical foundation for subsequent supervised analysis. However, while PCA maximizes sample differentiation, it does not specify whether these differences arise from within or between groups. To address this limitation, an OPLS-DA model was constructed. The OPLS-DA model showed excellent parameter performance ($R^2Y = 0.990$, $Q^2 = 0.991$ for grape samples; $R^2Y = 0.998$, $Q^2 = 0.986$ for wine samples), indicating its capacity to effectively differentiate different between samples and its strong predictive ability. The scoring plots in Fig. 4B and E clearly illustrate clear separations among the different grape cultivars. Through the substitution tests, the results confirmed that the model does not exhibit overfitting phenomenon (Fig. 4C and F), providing a reliability guarantee for the research results and enhancing the model's extensibility. In Variable Importance in Projection (VIP) analysis(Table S2 and Table S3), several significant phenolic compounds were identified, including Malvidin-3-O-glucoside, Petunidin-3-O-glucoside, (−) -epicatechin, (−)-Epigallocatechin, (−)-Gallocatechin, Isorhamnetin 3-O-glucoside, (−) -catechin, and so forth. The high rankings of these compounds across different wine grape cultivars, with VIP > 1.0 in the OPLS - DA model, suggest their crucial roles in the sensory properties and antioxidant capacity of the wines. Particularly, the elevated VIP value of 'Malvidin' and its derivatives underscores their significance in imparting color to the wine and enhancing its antioxidant properties. Totally, the combined use of PCA and OPLS-DA provides a comprehensive understanding of the phenolic profiles in grape and wine samples, facilitating the identification of key compounds that contribute to the quality and characteristics of the wines produced from different cultivars.

3.8. Correlation analysis

In this study, following the OPLS-DA analysis and replacement tests, we conducted a comprehensive examination of the correlation between phenolic compounds with a VIP value exceeding 1 and their physicochemical properties, as well as antioxidant capacity (Fig. 5; Table S4). Notably, anthocyanins emerge as the primary determinants of wine color. In vitro antioxidant activity demonstrated a strong relationship with non-anthocyanin flavonoids and anthocyanin compounds quantified by UPLC-MS^E. This correlation aligns with previous studies that utilized various assays based on electron transfer reactions, such as ABTS, FRAP, and DPPH (Heimler, Vignolini, Dini, Vincieri, & Romani, 2006). Specifically, the flavonol content measured by UPLC-MS^E method exhibited a significant correlation with antioxidant activity assessed by FRAP method with a linear correlation coefficient ($R^2 = 0.82$) in Fig. 5. This finding underscores the major role of polyphenols in antioxidant action. Numerous studies have reported a high correlation between total phenol content and antioxidant activity in red wine (Di Majo, La Guardia, Giammanco, La Neve, & Giammanco, 2008).

On specific compounds, (−)-Catechin showed a correlation with pH ($R^2 = 0.59$) and L* ($R^2 = 0.56$) in wine, changes in its concentration can influence the sensory properties of the wine by affecting acidity and color of the wine (Porgalı & Büyüktuncel, 2012). The results demonstrated that the correlation between Malvidin-3-O-glucoside and a (redness) reached 0.87329, highlighting its crucial influence on the red appearance of wine. Conversely, Delphinidin-3-O-glucoside exhibited a strong negative correlation with L (brightness) (−0.89646), indicating that increased levels of this compound will result in darker wine. These results are consistent with the behavior of anthocyanins under varying pH conditions, reinforcing their role in wine appearance.

The correlation between Flavanonols and FRAP was found to be 0.24468, suggesting that these flavonoids enhance antioxidant properties through electron transfer mechanisms. Although the correlations of (−) -catechin with ABTS and DPPH were relatively low (−0.06257 and − 0.36487, respectively) (Patel et al., 2016), it might act synergistically with other flavonoids to enhance the overall antioxidant potential of wine. The correlation between Delphinidin-3-O-glucoside and DPPH was 0.40143, signifying that Delphinidin-3-O-Glucoside has a strong free radical scavenging ability. Interestingly, Malvidin-3-O-glucoside was more inclined to contribute to color, showed a higher correlation with a (redness) and a lower correlation with antioxidant activity (FRAP) (−0.23954). This suggests that different modification groups of anthocyanin compounds may play distinct roles in antioxidant and color manifestation.

Flavonoids not only influence the antioxidant properties of wine but also regulate the flavor of wine through their contributions to astringency and bitterness. The positive correlation between Astilbin and FRAP (0.24468) indicates that while it enhances antioxidant capacity, it may also contribute to the wine's structure and complexity by imparting moderate astringency. Additionally, a negative correlation between L (brightness) and DPPH (−0.86446) suggests that darker wines possess stronger antioxidant properties, consistent with the observation that darker wines typically have higher levels of anthocyanins and

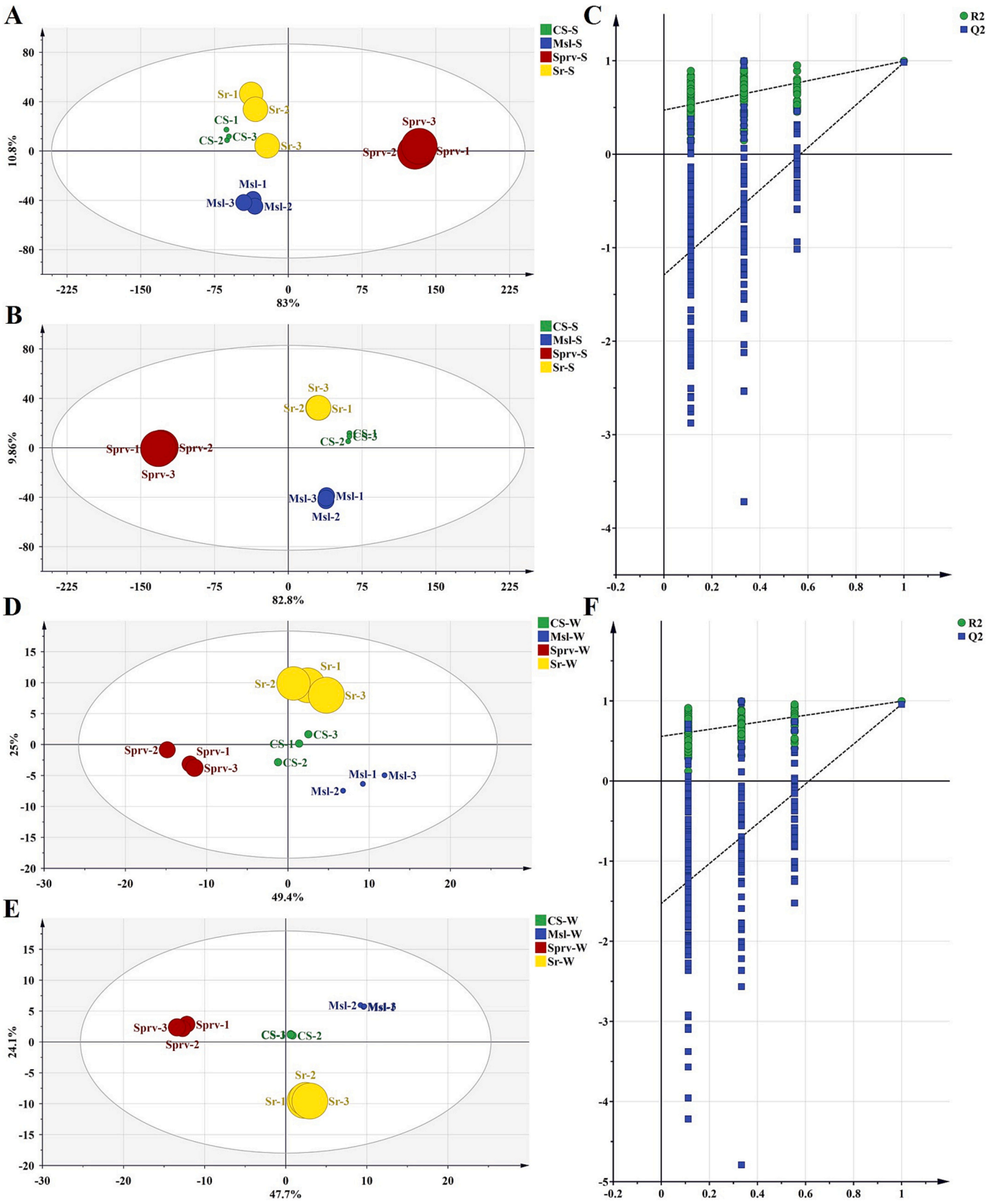

Fig. 4. PCA score plots of grape (A) and wine (D) samples from different cultivars, OPLS-DA score plots of grape (B) and wine (E) samples, OPLS-DA model permutation test plots of grape (C) and wine (F) samples. CS-S: phenolic compound extract of Cabernet Sauvignon skin; Msl-S: phenolic compound extract of Marselan skin; Sprv-S: phenolic compound extract of Saperavi skin; Sr-S: phenolic compound extract of Syrah skin; CS-W: phenolic compound extract of Cabernet Sauvignon wine; Msl-W: phenolic compound extract of Marselan wine; Sprv-W: phenolic compound extract of Saperavi wine; Sr-W: phenolic compound extract of Syrah wine.

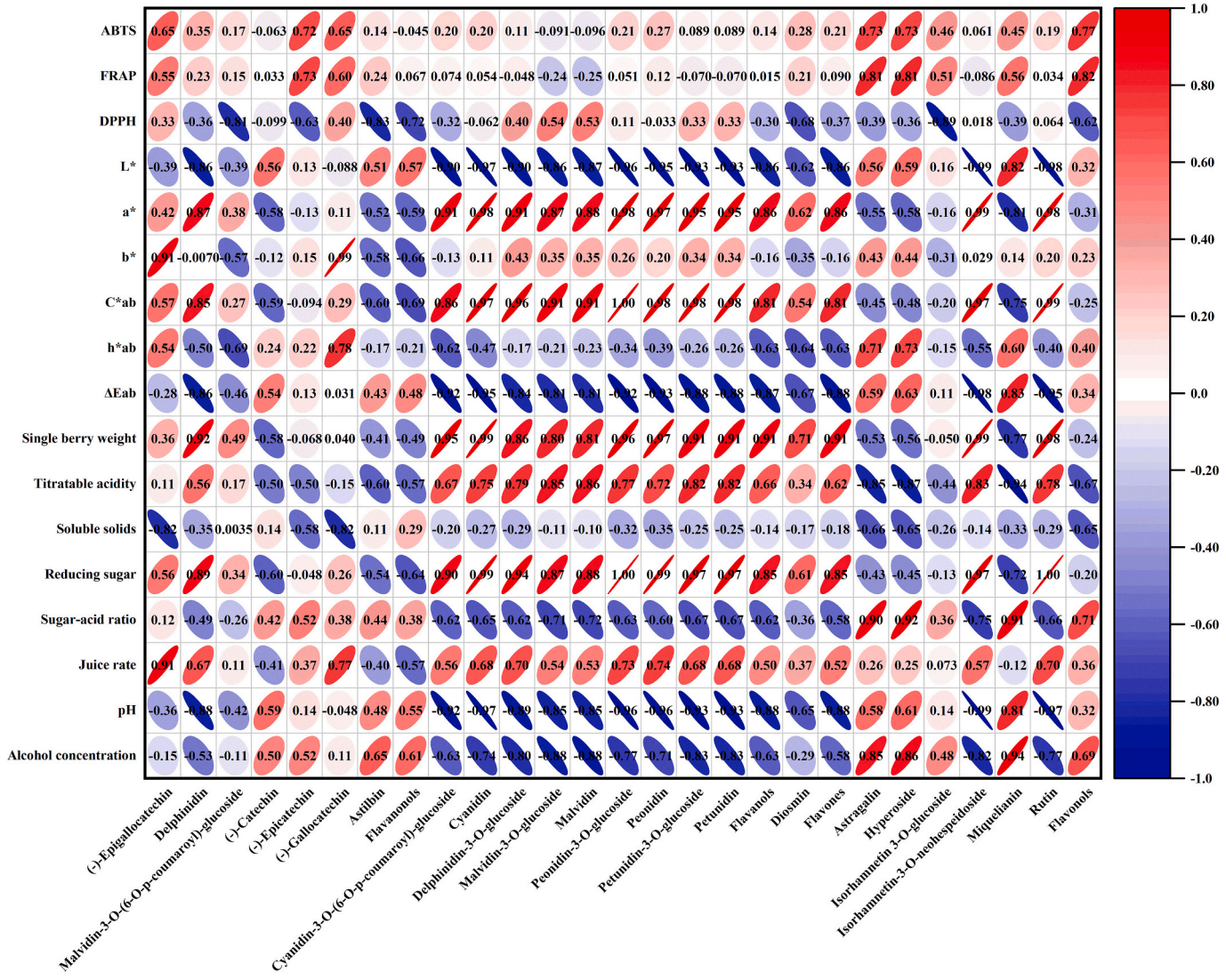

Fig. 5. The correlation among physicochemical indexes, CIELAB color space parameters and antioxidant activity with phenolic substances. The correlation between different anthocyanins is established through the differentiation of color attributes.

flavonoids.

These results reveal the intricate interactions among various compounds in grapes and wine. Anthocyanins and flavonoids not only enhance wine quality by directly influencing its color and antioxidant properties but also enrich the sensory experience by affecting flavor and balancing sweetness and acidity. This comprehensive understanding of phenolic compounds is essential for optimizing wine production and improving overall wine quality.

4. Conclusions

This study provides a comprehensive analysis of the phenolic profiles, antioxidant properties, and key physicochemical characteristics of four wine grape cultivars—Cabernet Sauvignon, Marselan, Saperavi, and Syrah—cultivated under the extreme conditions of the Turpan Basin, one of the hottest wine regions globally. By utilizing UPLC-MS^E and multiple antioxidant assays, we identified 43 anthocyanins and 66 non-anthocyanin flavonoids, revealing significant differences in phenolic composition, color intensity, and antioxidant potential among these cultivars. Saperavi exhibited the highest anthocyanin content, contributing to its intense coloration and robust antioxidant capacity, thus making it particularly well-suited for producing wines with enhanced stability and aging potential. Cabernet Sauvignon exhibited the strongest overall antioxidant activity, indicating its potential for producing wines with high oxidative stability. Additionally, the analysis of physicochemical parameters indicated that Saperavi exhibited the largest berry weight, juice yield, and acidity, underscoring its adaptability to heat stress, while Marselan's high soluble solids content and balanced sugar-acid ratio render it promising for high-alcohol wines. The color analysis further demonstrated that Saperavi and Syrah produced deeply saturated hues, reflecting high levels of anthocyanins and flavonoids, while also exhibited strong anthocyanin retention.

These findings offer critical insights into how extreme environmental conditions influence grape cultivar performance, providing a valuable foundation for selecting grape varieties that are best suited for wine production in high-temperature, arid regions. This study also contributes to a deeper understanding of the unique terroir characteristics of Turpan, highlighting the potential of these cultivars to produce high-quality wines with distinct regional attributes. Future studies could investigate how different viticultural and winemaking practices impact phenolic retention and stability, as well as explore the health-related benefits of these bioactive compounds. Such research would enhance our understanding of how environmental stressors shape the unique qualities of Turpan wines and improve their potential bioactive benefits.

Funding

This work was supported by the Xinjiang Uygur Autonomous Region Special Training for Ethnic Minorities Project (2022D03033); the Key R&D program of Xinjiang Uygur Autonomous Region (2024B02021–2); "Three Rural" Backbone Personnel Training Project of Xinjiang Uygur Autonomous Region (2023SNGGNT062); Tianshan Talent Project in Xinjiang Uygur Autonomous Region, Xinjiang Uygur Autonomous Region Tianshan Talents Training Program Young top-notch scientific and technological talents (2022TSYCJC0036); Xinjiang Tianshan Talents Training Program (2023TSYCCX0027).

CRediT authorship contribution statement

Shijian Bai: Writing – review & editing, Writing – original draft, Visualization, Validation, Supervision, Software, Resources, Project administration, Methodology, Investigation, Funding acquisition, Formal analysis, Data curation, Conceptualization. **Xiaoqing Tao:** Writing – review & editing, Writing – original draft, Visualization, Software, Methodology, Formal analysis, Data curation, Conceptualization. **Jinge Hu:** Writing – review & editing, Writing – original draft, Visualization, Validation, Supervision, Software, Resources, Project administration, Methodology, Investigation, Funding acquisition, Formal analysis, Data curation, Conceptualization. **Huawei Chen:** Investigation, Data curation. **Jiuyun Wu:** Investigation. **Fuchun Zhang:** Investigation. **Junshe Cai:** Investigation. **Guohong Wu:** Writing – review & editing, Supervision, Project administration, Funding acquisition. **Jiangfei Meng:** Writing – review & editing, Supervision, Project administration, Funding acquisition, Conceptualization.

Declaration of competing interest

The authors declare that they have no known competing financial interests or personal relationships that could have appeared to influence the work reported in this paper.

Appendix A. Supplementary data

Supplementary data to this article can be found online at https://doi.org/10.1016/j.fochx.2025.102301.

Data availability

Data will be made available on request.

References

Abe, L. T., Da Mota, R. V., Lajolo, F. M., & Genovese, M. I. (2007). Phenolic compounds and antioxidant activity of Vitis labrusca and Vitis vinfiera cultivars. *Ciencia E Tecnologia De Alimentos, 27*(2), 394–400. https://doi.org/10.1590/s0101-20612007000200032

Boulton, R. (2001). The copigmentation of anthocyanins and its role in the color of red wine: A critical review. *American Journal of Enology and Viticulture, 52*(2), 67–87.

Boulton, R. J. A. J. O. E., & viticulture. (2001). The copigmentation of anthocyanins and its role in the color of red wine: A critical review. *American Journal of Enology and Viticulture, 52*(2), 67–87.

Castillo-Muñoz, N., Gómez-Alonso, S., García-Romero, E., Hermosín-Gutiérrez, I. J. J. O. A., & chemistry, f. (2007). Flavonol profiles of *Vitis vinifera* red grapes and their single-cultivar wines. *Journal of Agricultural and Food Chemistry, 55*(3), 992–1002.

Cheynier, V., Duenas-Paton, M., Salas, E., Maury, C., Souquet, J.-M., Sarni-Manchado, P., & Viticulture.. (2006). Structure and properties of wine pigments and tannins. *American Journal of Enology and Viticulture, 57*(3), 298–305.

Cohen, S. D., Tarara, J. M., Kennedy, J. A. J. A., & c. a.. (2008). Assessing the impact of temperature on grape phenolic metabolism. *Analytica Chimica Acta, 621*(1), 57–67.

Cola, G., Failla, O., Maghradze, D., Megrelidze, L., & Mariani, L. (2017). Grapevine phenology and climate change in Georgia. *International Journal of Biometeorology, 61*(4), 761–773. https://doi.org/10.1007/s00484-016-1241-9

Czibulya, Z., Horváth, I., Kollár, L., Nikfardjam, M. P., & Kunsági-Máté, S. (2015). The effect of temperature, pH, and ionic strength on color stability of red wine. *Tetrahedron, 71*(20), 3027–3031. https://doi.org/10.1016/j.tet.2015.01.036

Di Majo, D., La Guardia, M., Giammanco, S., La Neve, L., & Giammanco, M. (2008). The antioxidant capacity of red wine in relationship with its polyphenolic constituents. Food Chemistry, 111(1), 45–49. doi:https://doi.org/10.1016/j.foodchem.2008.03.037.

Halliwell, B. J. N., & r.. (2012). Free radicals and antioxidants: updating a personal view. *Nutrition Reviews, 70*(5), 257–265.

Hanlin, R., Hrmova, M., Harbertson, J. F., Downey, M. O. J. A. J. O. G., & Research, W. (2010). Condensed tannin and grape cell wall interactions and their impact on tannin extractability into wine. *Australian Journal of Grape and Wine Research, 16*(1), 173–188.

He, F., Liang, N.-N., Mu, L., Pan, Q.-H., Wang, J., Reeves, M. J., & Duan, C.-Q. J. M. (2012a). Anthocyanins and their variation in red wines I. Monomeric anthocyanins and their color expression. *Molecules, 17*(2), 1571–1601.

He, F., Liang, N.-N., Mu, L., Pan, Q.-H., Wang, J., Reeves, M. J., & Duan, C.-Q. J. M. (2012b). Anthocyanins and their variation in red wines II. Anthocyanin derived pigments and their color evolution. *Molecules, 17*(2), 1483–1519.

Heimler, D., Vignolini, P., Dini, M. G., Vincieri, F. F., & Romani, A. (2006). Antiradical activity and polyphenol composition of local Brassicaceae edible varieties. *Food Chemistry, 99*(3), 464–469. https://doi.org/10.1016/j.foodchem.2005.07.057

Ieri, F., Campo, M., Cassiani, C., Urciuoli, S., Jurkhadze, K., & Romani, A. (2021). Analysis of aroma and polyphenolic compounds in Saperavi red wine vinified in Qvevri. *Food Science & Nutrition, 9*(12), 6492–6500. https://doi.org/10.1002/fsn3.2556

Jackson, R. S. (2008). *Wine science: Principles and applications: Academic press*.

Ju, Y., Yang, L., Yue, X., Li, Y., He, R., Deng, S., & Wellness, H. (2021). Anthocyanin profiles and color properties of red wines made from Vitis davidii and *Vitis vinifera* grapes. *Food Science and Human Wellness, 10*(3), 335–344.

Kennedy, J. A., Saucier, C., & Glories, Y. (2006). Grape and wine phenolics: History and perspective. *American Journal of Enology and Viticulture, 57*(3), 239–248. ://WOS:000240934100001.

Kumar, L., Tian, B., & Harrison, R. J. L. (2022). Interactions of *Vitis vinifera* L. cv. Pinot Noir grape anthocyanins with seed proanthocyanidins and their effect on wine color and phenolic composition. *LWT, 162*, Article 113428.

Lecourieux, F., Kappel, C., Pieri, P., Charon, J., Pillet, J., Hilbert, G., … i. P. S.. (2017). Dissecting the biochemical and transcriptomic effects of a locally applied heat treatment on developing Cabernet Sauvignon grape berries. *Frontiers in Plant Science, 8*, 53.

Li, N., Li, G., Guan, X., Li, A., & Tao, Y. (2025). Volatile aroma compound-based decoding and prediction of sweet berry aromas in dry red wine. *Food Chemistry, 463*(Pt 2), Article 141248. https://doi.org/10.1016/j.foodchem.2024.141248

Lingua, M. S., Fabani, M. P., Wunderlin, D. A., & Baroni, M. V. (2016). From grape to wine: Changes in phenolic composition and its influence on antioxidant activity. *Food Chemistry, 208*, 228–238. https://doi.org/10.1016/j.foodchem.2016.04.009

Mattivi, F., Guzzon, R., Vrhovsek, U., Stefanini, M., Velasco, R. J. J. O. A., & chemistry, f. (2006). Metabolite profiling of grape: flavonols and anthocyanins. *Comparative Study, 54*(20), 7692–7702.

Medina-Plaza, C., Dubois, A., Tomasino, E., & Oberholster, A. (2024). Effect of storing conditions (lighting, temperature and bottle color) on rose<acute accent> wine attributes. *Food Chemistry, 439*, 12. https://doi.org/10.1016/j.foodchem.2023.138032

Mezzatesta, D. S., Berli, F. J., Arancibia, C., Buscema, F. G., & Piccoli, P. N. (2022). Impact of contrasting soils in a high-altitude vineyard of *Vitis vinifera* L. cv. Malbec: root morphology and distribution, vegetative and reproductive expressions, and berry skin phenolics. *OENO one, 56*(2), 149–163. https://doi.org/10.20870/oeno-one.2022.56.2.4917

Mosedale, J. R., Wilson, R. J., & Maclean, I. M. D. (2015). Climate change and crop exposure to adverse weather: Changes to frost risk and grapevine flowering conditions. *PLoS One, 10*(10), 16. https://doi.org/10.1371/journal.pone.0141218

Patel, M. I., Wang, A. G., Kapphahn, K., Desai, M., Chlebowski, R. T., Simon, M. S., & Wakelee, H. A. (2016). Racial and ethnic variations in lung Cancer incidence and mortality: Results from the Women's Health Initiative. *Journal of Clinical Oncology, 34*(4). https://doi.org/10.1200/jco.2015.63.5789, 360-+.

Pérez-Magariño, S., & González-Sanjosé, M. L. (2003). Application of absorbance values used in wineries for estimating CIELAB parameters in red wines. *Food Chemistry, 81*(2), 301–306. https://doi.org/10.1016/s0308-8146(02)00509-5

Porgalı, E., & Büyüktuncel, E. (2012). Determination of phenolic composition and antioxidant capacity of native red wines by high performance liquid chromatography and spectrophotometric methods. *Food Research International, 45*(1), 145–154. https://doi.org/10.1016/j.foodres.2011.10.025

Re, R., Pellegrini, N., Proteggente, A., Pannala, A., Yang, M., Rice-Evans, C. J. F., & r. b., & medicine.. (1999). Antioxidant activity applying an improved ABTS radical cation decolorization assay. *Original Contributions, 26*(9–10), 1231–1237.

Rodríguez-Lorenzo, M., Mauri, N., Royo, C., Rambla, J. L., Diretto, G., Demurtas, O., … o. E. B.. (2023). The flavour of grape colour: anthocyanin content tunes aroma precursor composition by altering the berry microenvironment. *Journal of Experimental Botany, 74*(20), 6369–6390.

Sáenz Gamasa, C., Hernández, B., De Santiago, J. V., Alberdi, C., Alfonso, S., Diñeiro, J. M. J. E. F. R., & technology. (2009). Measurement of the colour of white and rosé wines in visual tasting conditions. 229, 263–276.

Santos, M. C. B., Lima, L. R. D., Nascimento, F. R., do Nascimento, T. P., Cameron, L. C., & Ferreira, M. S. L. (2019). Metabolomic approach for characterization of phenolic compounds in different wheat genotypes during grain development. *Food Research International, 124*, 118–128. https://doi.org/10.1016/j.foodres.2018.08.034

Savalekar, K., Shabeer, T. P. A., Khan, Z., Oulkar, D., Jain, P., Patil, C., & Banerjee, K. (2019). Targeted phenolic profiling of sauvignon blanc and shiraz grapes grown in two regions of India by liquid chromatography-tandem mass spectrometry. *Journal*

of Food Science and Technology-Mysore, 56(7), 3300–3312. https://doi.org/10.1007/s13197-019-03802-w

Teixeira, A., Eiras-Dias, J., Castellarin, S. D., & Gerós, H. J. I. J. O. M. S. (2013). Berry phenolics of grapevine under challenging environments. *International Journal of Molecular Sciences*, (9), 18711–18739.

Valentini, G., Pastore, C., Allegro, G., Mazzoleni, R., Chinnici, F., & Filippetti, I. (2022). Vine physiology, yield parameters and berry composition of Sangiovese grape under two different canopy shapes and irrigation regimes. *Agronomy-Basel, 12*(8), 18. https://doi.org/10.3390/agronomy12081967

Wang, H., Race, E. J., Shrikhande, A. J. J. J. O. A., & Chemistry, F. (2003). Characterization of anthocyanins in grape juices by ion trap liquid chromatography– mass spectrometry. *Journal of Agricultural and Food Chemistry, 51*(7), 1839–1844.

Yue, X., Zhao, Y., Ma, X., Jiao, X., Fang, Y., Zhang, Z., & Ju, Y. (2021). Effects of leaf removal on the accumulation of anthocyanins and the expression of anthocyanin biosynthetic genes in cabernet sauvignon (Vitis vinifera L.) grapes. *Journal of the Science of Food and Agriculture, 101*(8), 3214–3224. https://doi.org/10.1002/jsfa.10951

Zhang, Z., Tian, C. P., Zhang, Y., Li, C. Z. Y., Li, X., Yu, Q., & Feng, S. Q. (2020). Transcriptomic and metabolomic analysis provides insights into anthocyanin and procyanidin accumulation in pear. *BMC Plant Biology, 20*(1), 14. https://doi.org/10.1186/s12870-020-02344-0